Generation of 1-MHz, 64-W, 26-fs green pulses via SHG of nonlinearly compressed pulses at 1.03 μm

Dongliang Wang [1, 2], Qi Liu [3], Zhongchao Li [4], Xinyue Yuan[1, 2], Hongyue Wu[1, 2], Zixi Liu[5], Wei Liu [4], and Guoqing Chang [1, 2, 6]

[1]*Beijing National Laboratory for Condensed Matter Physics, Institute of Physics, Chinese Academy of Sciences, Beijing 100190, China*
[2]*University of Chinese Academy of Sciences, Beijing 100049, China*
[3]*Institute of Advanced Light Source Facilities, Shenzhen 518049, China*
[4]*School of Science, Sun Yat-Sen University, Shenzhen 518107, China*
[5]*School of Physics, Nankai University, Tianjin, 300071, China*
[6]*Songshan Lake Materials Laboratory, Dongguan, Guangdong 523808, China*
Corresponding authors: liuwei95@mail.sysu.edu.cn, guoqing.chang@iphy.ac.cn

Abstract High-order harmonic generation (HHG) in noble gases driven by femtosecond lasers is currently a feasible solution to obtain ultrafast pulses in the extreme ultraviolet (EUV) wavelength range. Implementation of high-flux EUV sources requires driving HHG using an ultrafast laser source at the visible wavelength range with MHz repetition-rate. In this paper, we employ a multi-pass cell followed by chirped mirrors to compress 1-MHz, 200-W, 300-fs pulses at 1.03 μm to a duration of 35 fs. The resulting 186-W compressed pulses are focused onto 0.5-mm thick BBO crystal to drive second harmonic generation and produce positively chirped pulses at 520 nm. These green pulses are dechirped to 26 fs in

This peer-reviewed article has been accepted for publication but not yet copyedited or typeset, and so may be subject to change during the production process. The article is considered published and may be cited using its DOI.

This is an Open Access article, distributed under the terms of the Creative Commons Attribution licence (https://creativecommons.org/licenses/by/4.0/), which permits unrestricted re-use, distribution, and reproduction in any medium, provided the original work is properly cited.

10.1017/hpl.2025.10056

duration with an average power of 64 W, which, to the best of our knowledge, represents the highest average power of green pulses with the duration below 100 fs.

Key words: ultrafast lasers, nonlinear compressor, second harmonic generation

1. INTRODUCTION

Ultrafast extreme ultraviolet (EUV, 10-120 nm) sources with high average power are desired by many scientific applications, such as EUV absorption spectroscopy, EUV-ionization spectroscopy, and coherent diffractive imaging of ultrafast magnetization dynamics. For instance, higher EUV power can alleviate space-charge limitations in photoelectron emission spectroscopy at elevated repetition rates [1], while simultaneously reducing data collection durations and improving signal-to-noise ratios in time-resolved coincidence measurements. High-order harmonic generation (HHG) in noble gases driven by femtosecond lasers is currently a feasible solution to implement ultrafast EUV sources [2, 3]. Since HHG efficiency is highly dependent on the driving laser wavelength known as $\eta \propto \lambda^{-(5\text{-}6)}$ [4], using a driving ultrafast laser at a shorter wavelength laser can significantly improve the HHG yield and produce mW-level EUV pulses [5-7]. With all other parameters fixed, increasing the driving-laser repetition rate from kHz to MHz can substantially scale up the average power of the resulting EUV source as well.

Ultrafast Ti:Sapphire lasers (centered at ~800 nm) are widely employed for driving HHG. However, limited by the lower repetition rate (normally 1-10 kHz), the

https://doi.org/10.1017/hpl.2025.10056 Published online by Cambridge University Press

generated EUV source is below 100 μW per harmonic line [8]. Further power scaling is hindered by the challenges in thermal management of Ti:Sapphire crystal required for increasing the repetition rate. In contrast, ultrafast Yb-doped lasers offer superior thermal dissipation and can operate with average power much higher than can be achieved by Ti:Sapphire lasers, positioning them as a promising alternative for advancing HHG power [9]. Notably, Yb-doped rod-type fiber systems currently hold the record for generating >10 kW average power in ultrafast laser systems while simultaneously maintaining excellent beam quality [10]. Ultrafast Yb-doped lasers usually emit pulses at ~1.03 μm with a duration longer than 100 fs [11]. To efficiently driving HHG, conversion of these pulses to a shorter wavelength with a much shorter duration (e.g. <30 fs) is implemented via second-harmonic generation (SHG) in conjunction with pulse post-compression. Figure 1 summarizes the representative results of the current femtosecond sources at the green wavelength range derived from ultrafast Yb-doped lasers. Depending on the sequence of SHG and pulse compression, two main approaches exist to produce energetic femtosecond pulses in the green wavelength range:

(1) Relatively long (>100 fs) green pulses are first generated by SHG and then post compressed to a much shorter duration. Because the 1.03-μm pulses have a narrow bandwidth (i.e., <10 nm), a thicker SHG crystal can be employed leading to higher conversion efficiency. The generated SHG pulses have a similar duration as the 1.03-μm pulses. To shorten the pulse duration, the SHG pulses are spectrally broadened in a certain medium—such as multiple thin

https://doi.org/10.1017/hpl.2025.10056 Published online by Cambridge University Press

plates (MTPs), hollow-core fiber (HCF), and gas-filled multi-pass cell (MPC)—prior to phase compensation by chirped mirrors. The MTP compression features high efficiency while it is only suited for pulse energy below 100 μJ [12]. Gas-filled HCFs can handle mJ pulse-energy despite of a relatively low efficiency (<60%) [7, 13, 14]. For example, Descamps et al. employed HCF for green pulse compression and obtained 15-fs pulses with up to 11.5-W average power; However, due to the 57% compression efficiency of the HCF, the overall system efficiency was only 23% [14]. Using similar approach, Klas et al. employed a Yb-fiber laser with higher average power and achieved 19-fs green pulses at 51 W with a system efficiency of 27% [7]. Further power scaling necessitates active cooling of the fiber and stabilization of the input beam pointing to prevent HCF damage [15, 16]. MPC has been widely adopted to compress mJ-level pulses at 1.03 μm with average power exceeding 1 kW [17]. When applied to green pulses, MPC has a high efficiency (>85%) as well [18, 19]. However, the relatively low damage threshold of optical components at the green wavelength rage requires a much larger beam on the MPC cavity mirrors, which increases the overall footprint and complexity of the system. For example, the MPC cavity length when dealing with green pulses of ~0.5 mJ energy was close to 2 m [19].

Before compression, the green pulses directly generated from SHG of 1.03-μm have a typical duration of 200-300 fs. Currently, chirped mirrors with large group-delay dispersion (GDD) (>500 fs^2) are absent in the green

https://doi.org/10.1017/hpl.2025.10056 Published online by Cambridge University Press

wavelength range. As a result, more than 15 reflections are usually required to dechirp the spectrally broadened green pulses, which causes power loss and degrades the compression quality.

(2) The 1.03-μm pulses are compressed first to a much shorter duration and followed by SHG to obtain green pulses. The compressed 1.03-μm pulses possess a broader bandwidth, and thus a thinner SHG crystal has to be used in order to convert the full bandwidth. For example, Tenyakov et al. used HCF to spectrally broaden 1.03-μm pulses and KDP crystal for SHG [20, 21]. After dechirping the green pulses with a prism pair, they obtained 15-fs pulses with up to 45-μJ energy; however, the average power was only 0.45 W. Klas et al. employed BBO crystal for SHG and obtained 90-μJ pulses with up to 11-W average power; however, the pulse duration was 85 fs and overall efficiency was only 9% [5].

https://doi.org/10.1017/hpl.2025.10056 Published online by Cambridge University Press

Figure 1. Representative experimental results on generation of green pulses.

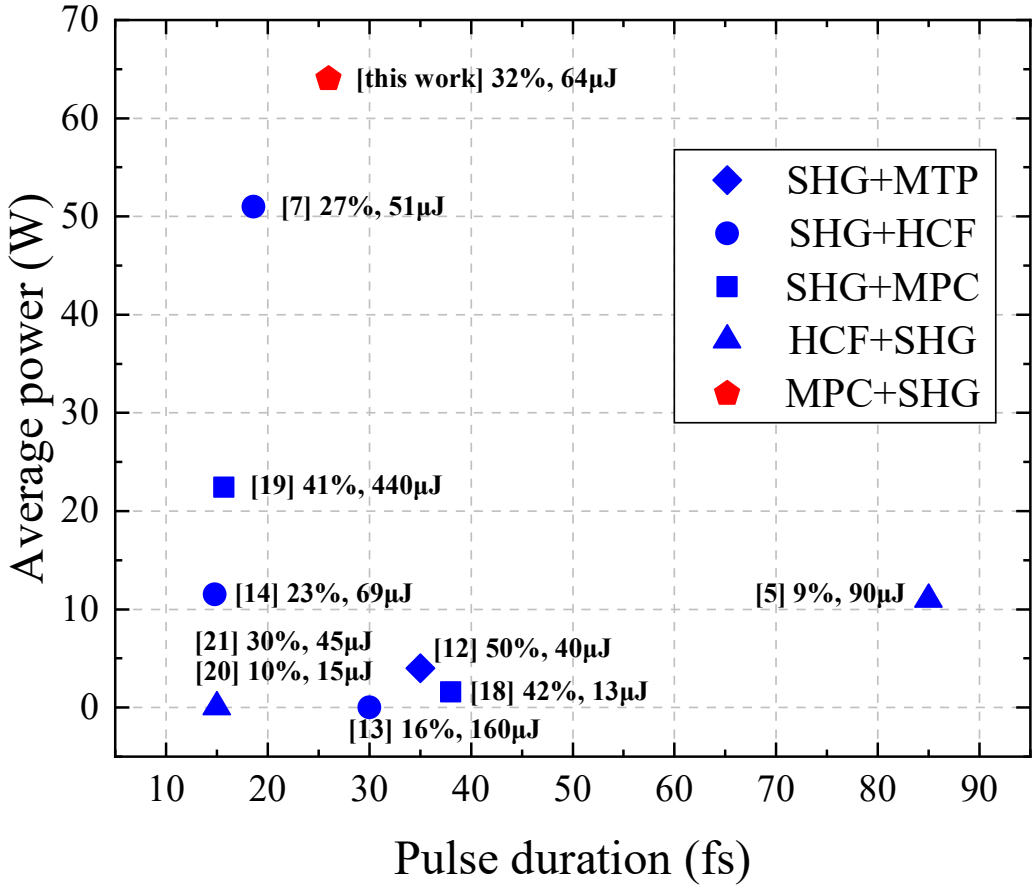

In this paper, we employ MPC to shorten the 1.03-μm pulses delivered by a Yb-fiber laser system, and then use BBO crystal for SHG. Compared with KDP crystal, BBO features thermal robustness, large nonlinear coefficient, and low pulse temporal walk-off [22]. Consequently, our system produces 1-MHz, 64-W, 26-fs pulses centered at 520 nm with a total efficiency of 32%, which, to the best of our knowledge, represents the highest average power of green pulses with the duration below 100 fs.

2. Experimental Setup

Figure 2 illustrates our experimental setup. The rod-type Yb-fiber laser system emits

https://doi.org/10.1017/hpl.2025.10056 Published online by Cambridge University Press

1-MHz, 230-fs pulses centered at 1.03 μm with 200-W average power (corresponding to 200-μJ pulse energy) [23]. The laser beam is mode matched to the eigenmode of a MPC via three lenses (with focal length of 100 mm, -200 mm, and 300 mm) to ensure identical beam properties per pass through the cell. The enclosed Herriot-type MPC consists of two identical low-dispersion mirrors (0.3 m in radius of curvature and 50.8 mm in diameter) separated by 0.586 m. The calculated Gaussian eigenmode has a $1/e^2$ diameter of 0.24 mm at the focal plane and 1.6 mm on the mirrors. The MPC is filled with 3-bar krypton gas and the pulse spectrum is significantly broadened after 23 focal passes. Matching the collimated beam to the linear eigenmode of the MPC and re-collimating the beam after passing through the cell is realized by one plano-convex lens (focal length of 800 mm). After the MPC, the spectrally broadened pulses with 186-W average power are de-chirped by 4 chirped mirrors which provide a total GDD of -3500 fs^2. The de-chirped pulses are reduced to 2.5 mm in beam diameter by a combination of a L5 lens (150-mm focal length) and a L6 lens (-75-mm focal length).

https://doi.org/10.1017/hpl.2025.10056 Published online by Cambridge University Press

Figure 2. Schematic of the experimental setup. L: lens, HR: high-reflection mirror, CM: chirped mirror, BBO: nonlinear crystal, DM: dichroic mirror, FS: fused silica.

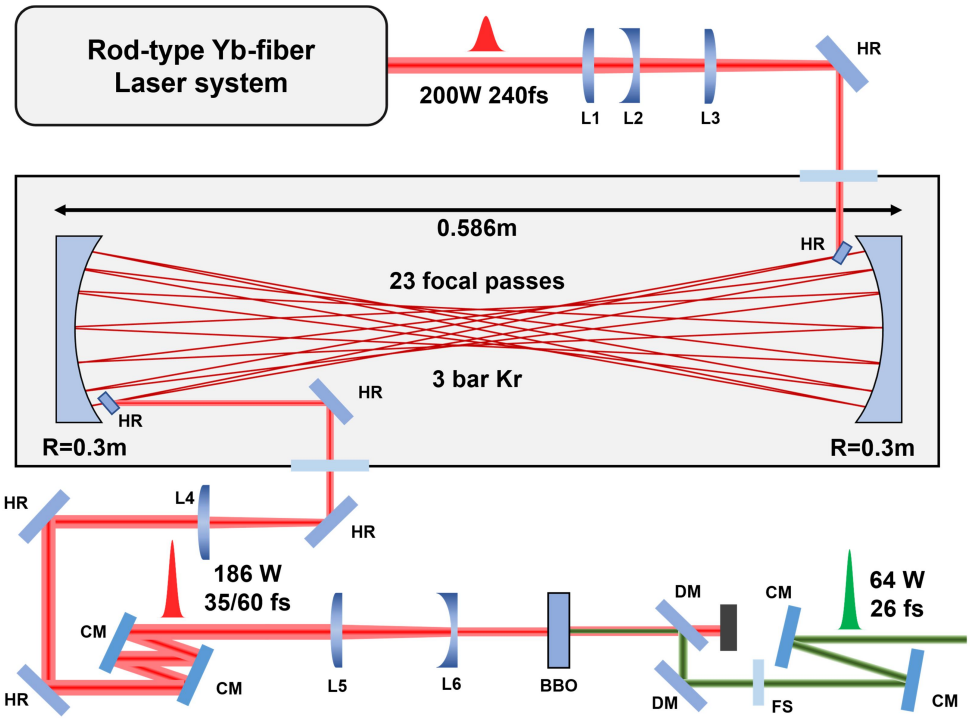

Efficient generation of green pulses via SHG from 1.03-μm femtosecond pulses at 186 W needs a careful selection of proper nonlinear crystal. In the small-signal model without considering depletion of the fundamental wave, SHG efficiency can be estimated as

$$\eta = \frac{8\pi^2 d_{eff}^2 L^2 I_\omega}{\varepsilon_0 c^3 n_\omega^2 n_{2\omega} \lambda_\omega^2} \cdot sinc^2(\frac{\Delta kL}{2}),$$

where η is the SHG efficiency, d_{eff} the effective nonlinear coefficient, L the the crystal thickness, I_ω the intensity at fundamental frequency. $\Delta k = 2k_\omega - k_{2\omega}$ is the phase mismatch at central frequencies. n_ω and $n_{2\omega}$ are the refractive indices of the corresponding frequencies, and λ_ω is the fundamental wavelength. To quantify the dependence of SHG efficiency on the nonlinear crystal, a figure of merit can be

https://doi.org/10.1017/hpl.2025.10056 Published online by Cambridge University Press

defined as $\mathrm{FOM} = \frac{8\pi^2 d_{eff}^2 L^2}{n_\omega^2 n_{2\omega}} \cdot sinc^2(\frac{\Delta kL}{2})$.

Table 1 presents a comparison of optical properties of seven crystals commonly used for SHG. For frequency doubling of high-power broadband (>40 nm) femtosecond pulses at 1.03 μm, the crystal thickness is usually less than 1 mm to provide enough phase-matching bandwidth. In this scenario, spatial walk-off between the input pulses and the SHG pulses is minimal and thus not included in the table. Column 3-6 lists effective nonlinear coefficient (d_{eff}), phase-matching bandwidth (PB), temporal walk-off (TW), and temperature tolerance (TT). Temperature tolerance is defined as the ratio between the temperature change and the wave-vector mismatch, which quantifies the variation of phase mismatch due to temperature rise in crystal. A crystal with larger temperature tolerance is beneficial when applied to SHG of femtosecond pulses with high average power (i.e., >100 W).

An ideal SHG crystal should simultaneously exhibit low temporal walk-off, large d_{eff}, broad phase-matching bandwidth, and large temperature tolerance. To have a fair comparison, we calculate the FOM of the listed crystals for frequency doubling of 30-fs pulses centered at 1.03 μm (Spectral bandwidth is about 14200 GHz). L is estimated as $\mathrm{PB}/14200$. We assume that Δk is caused by a temperature rise of 30 K, i.e., $\Delta k = 30/\mathrm{TT}$. The last column in Table 1 shows the calculated FOM for each crystal. BBO crystal exhibits the largest FOM; together with a high damage threshold, BBO crystal is good choice for frequency doubling high-power femtosecond pulses with a broad bandwidth. KDP has a comparable FOM as BBO; however, KDP crystal features a damage threshold two orders of magnitude lower compared with BBO

https://doi.org/10.1017/hpl.2025.10056 Published online by Cambridge University Press

crystal [24]. The SHG average power obtained based on KDP crystals is usually < 1 W.

Table 1. Comparison of SHG performance among typical nonlinear crystals. PT: Phase-matching Type; d_{eff}: effective nonlinear coefficient; PB: Phase-matching Bandwidth; TW: Temporal walk-off; TT: temperature tolerance; $\mathrm{FOM} = \frac{8\pi^2 d_{eff}^2 L^2}{n_\omega^2 n_{2\omega}} \cdot sinc^2(\frac{\Delta kL}{2})$. (PB and temperatures are ranges over which (LΔk) varies from -π to π. This is 13% greater than the full width at half maximum for the sinc^2 (ΔkL/2) function that describes SHG efficiency. λ_ω = 1030 nm, $\lambda_{2\omega}$ = 515 nm, T=300K)

Crystal	PT	d_{eff} (pm/V)	PB (GHz·cm)	TW (fs/mm)	TT (K·cm)	FOM (10^{18}·pm^3/V^2)
BBO	oo→e	2.01	527	93	37.7	3.44
LBO	oo→e	0.83	971	53	7.02	2.06
BIBO	ee→o	3.40	260	193	2.68	1.77
KDP	oo→e	0.27	37677	1.3	11.2	3.31
KTP	eo→e	2.80	110/384	458/134	40.7	2.50
CLBO	oo→e	0.39	1090	47	53.6	0.78
CBO	ee→o	1.01	634	80	109.6	1.54

We calculate the conversion efficiency at various crystal thicknesses by numerically solving the coupled-wave equations for frequency doubling 1.03-μm, 30-fs pulses with 185-μJ pulse energy and 3-mm beam diameter in BBO crystal. The red curve in Fig. 3 shows the conversion efficiency as a function of BBO thickness, and the black curve shows the corresponding phase-matching bandwidth. As expected, increasing the crystal thickness improves the SHG efficiency accompanied by a

https://doi.org/10.1017/hpl.2025.10056 Published online by Cambridge University Press

reduced phase-matching bandwidth. A 0.5-mm thick BBO crystal (indicated by the gray dashed line) appears to be an optimal choice because it provides enough phase-matching bandwidth (36 nm) to support green pulses with <30 fs duration; meanwhile, it corresponds to a high conversion efficiency of 37%. Guided by above analysis, we experimentally choose a 0.5-mm-thick BBO crystal to perform SHG followed by completely separating the SHG pulses from the input 1.03-μm pulses using dichroic mirrors.

Figure 3. Phase-matching bandwidth (black) and SHG efficiency (red) versus BBO thickness. Gray dotted line marks the phase matching bandwidth and SHG efficiency of 0.5-mm thick BBO.

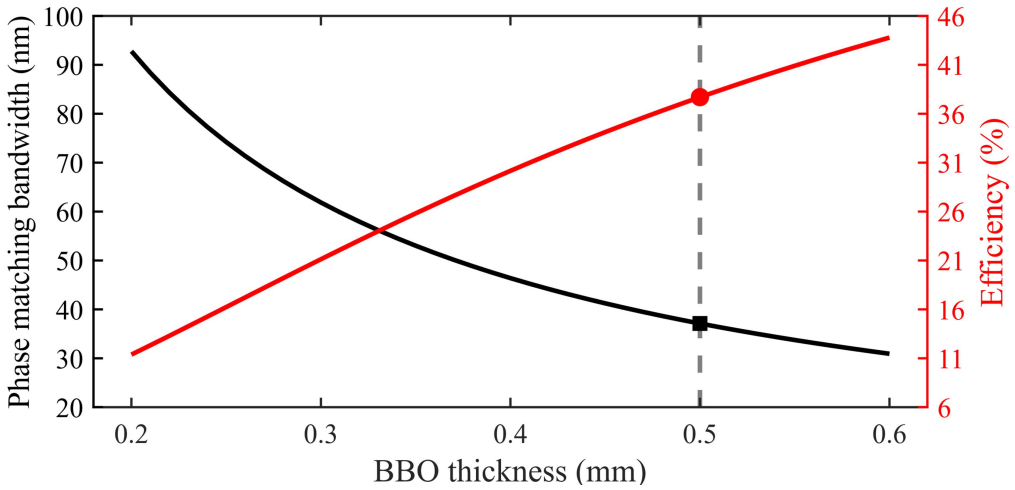

3. Results and Discussion

As the pulse propagates inside the MPC, the accumulated nonlinear phase—which is proportional to the pulse energy and the nonlinear coefficient (or gas pressure)—results in a broadened optical spectrum that in turn determines the transform-limited (TL) pulse duration [25]. Figure 4(a) plots the broadened spectra at

https://doi.org/10.1017/hpl.2025.10056 Published online by Cambridge University Press

the MPC output measured at 100 μJ with the Kr pressure increased from 1.5 bar to 4.5 bar (with interval of 0.5 bar). As Fig. 4(b) shows, the corresponding TL pulse duration calculated from the measured spectra drops from 130 fs to 53 fs. In another experiment, we fix the Kr pressure at 3 Bar and measure the broadened spectra with the pulse energy increased from 50 μJ to 200 μJ [Fig. 4(c)]; the corresponding TL pulse duration decreases from 126 fs to 31 fs [Fig. 4(d)].

Figure 4. Broadened spectra and TL pulse duration at different pressures and input energies. Broadened spectra (a) and TL pulse duration (b) at 1.5-4. 5 bar Kr pressure at 100 μJ input energy, broadened spectra (c) and TL pulse duration (d) at 50-200 μJ input energy at 3 bar pressure.

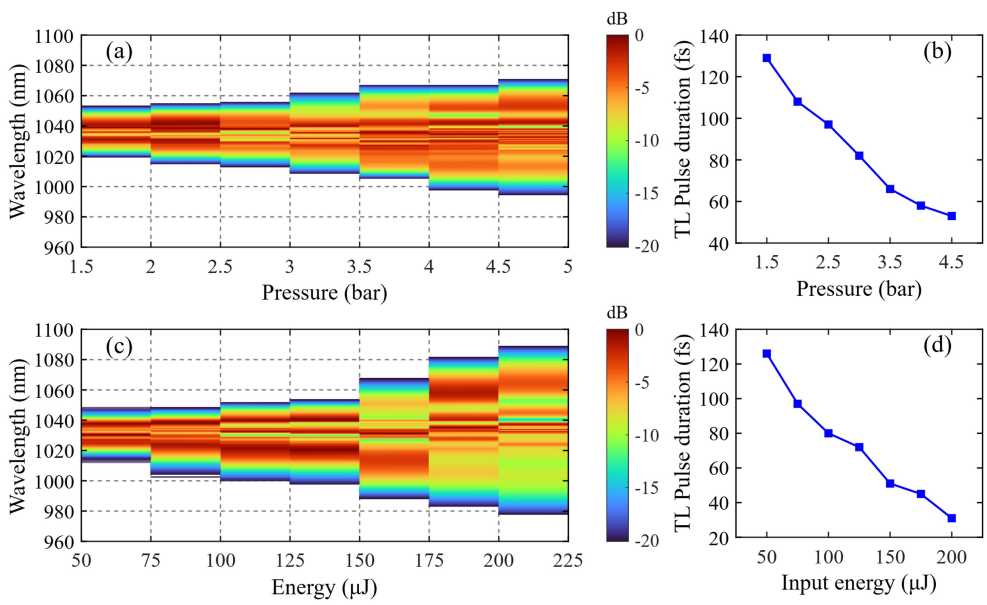

The peak power on the concave mirror of the MPC is up to 200 GW/cm^2, well below the damage threshold. Figure 5(a) shows MPC output power and efficiency versus input power. At the highest input power of 200 W, the MPC output power is 186 W. The efficiency of the MPC is >90% at all powers. Due to a long optical path of 18.5 m, the optical beam at MPC output exhibits noticeable pointing fluctuation. To

https://doi.org/10.1017/hpl.2025.10056 Published online by Cambridge University Press

meet the requirement for driving HHG, we add a pointing stabilization device, which consists of two actuators and two 4-quadrant-diode detectors. The pointing results are shown in Fig. 5(b)-(c). The measurement uses a 200 mm lens to focus the spot, and the CCD camera samples at 5 Hz for 30 minutes. The root mean square (RMS) of the focal spot shift over 30 minutes is 1.5 μm and 0.8 μm. Horizontal and vertical RMS deviation is 7.6 μrad and 4.1 μrad, which represents about 2.6 times reduction compared with the case without pointing stabilization.

Figure 5. (a) MPC output power and efficiency versus input power. Horizontal (b) and vertical (c) beam angular pointing stability.

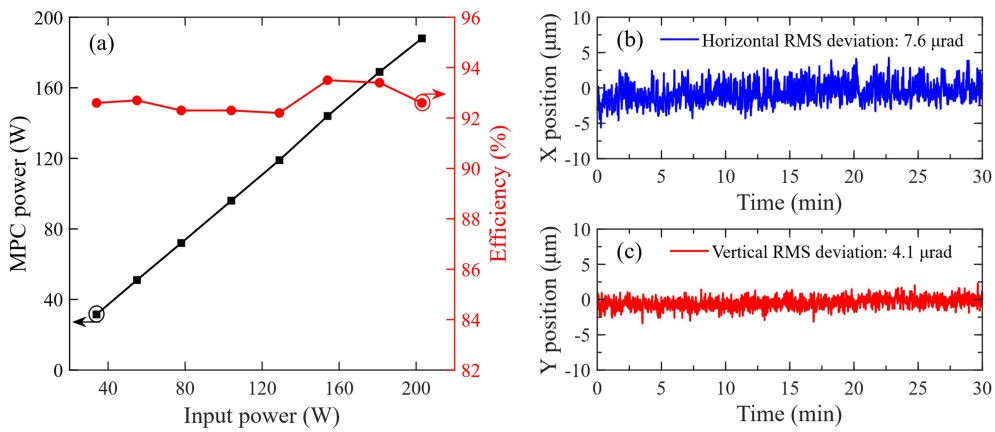

The red curve in Fig. 6(a) shows the MPC output spectrum at 200-W input power with the Kr pressure set at 3 bar (YOKOGAWA, AQ6370D, Resolution: 0.2 nm). The input spectrum with a spectral width of 8.1 nm [gray shading area in Fig. 6(a)] is significantly broadened spanning 980-1080 nm. The spectrally broadened pulses are then dechirped by chirped mirrors that provide -3500fs^2 GDD. The red curve in Fig. 6(b) plots the measured autocorrelation trace of the dechirped pulse with an estimated duration of 35 fs. Also plotted in the same figure is the calculated

https://doi.org/10.1017/hpl.2025.10056 Published online by Cambridge University Press

autocorrelation trace of the corresponding TL pulses (black dashed curve) with a duration of 31 fs, and the dechirped pulses are close to be transform-limited.

Figure 6. (a) Input (gray shading) and output (red) spectra of MPC. (b) Measured autocorrelation trace (red) and calculated autocorrelation trace of the TL pulse (black dashed).

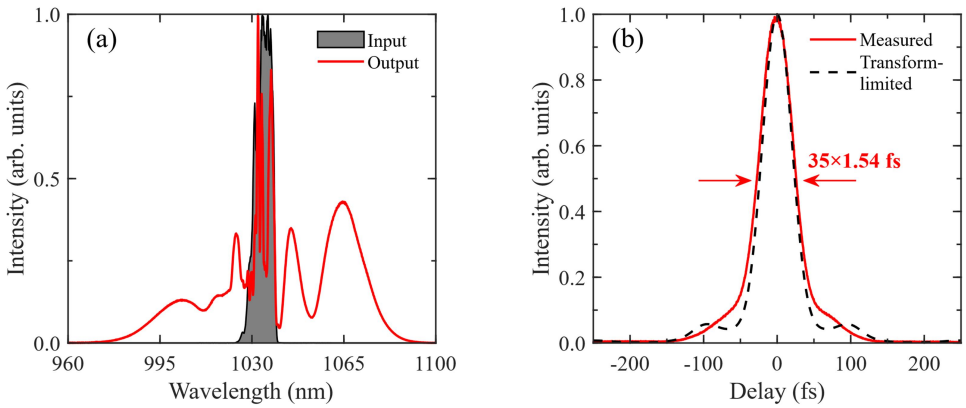

A 0.5 mm-thick BBO crystal cut for type-I phase matching (phase matching angle at 23.4°) is used to convert the 186-W compressed pulses to the green spectral range via SHG. The temporal walk-off between the 1.03-μm pulse and the SHG pulse in the BBO crystal is 93 fs/mm, which reduces the conversion efficiency and narrows the SHG spectrum. This adverse effect can be mitigated by slightly pre-chirping the input 1.03-μm pulse. In our experiments, we intentionally add ~400 fs^2 GDD to the 1.03-μm compressed pulse [i.e., the measured pulse in Fig. 6(b)] in order to stretch it to a duration of about 60 fs. For type-I SHG at 1030 nm in a 0.5-mm BBO crystal, the walk-off angle of 57 mrad yields a spatial displacement of ~0.03 mm between the fundamental and SHG beams. Such a displacement is negligible relative to the fundamental beam diameter of 2.5 mm, which has little impact on the conversion

https://doi.org/10.1017/hpl.2025.10056 Published online by Cambridge University Press

efficiency. In this scenario, the resulting SHG pulses have 66-W average power (corresponding to 36% conversion efficiency) with a duration of 78 fs; inset of Fig. 7(a) shows the SHG spectrum with a spectral width of 18 nm (AVANTES, AvaSpec-3648, Resolution: 0.33 nm). The SHG pulses are compressed by two chirped mirrors designed to provide -100-fs^2 GDD per reflection over the spectral range from 490 nm to 540 nm. The compressed pulse duration drops from 78 fs to 60 fs (32 fs) corresponding to the compensated GDD at -200 fs^2 (-400 fs^2). To achieve the shortest pulse duration, we place a 2-mm-thick fused-silica plate before the chirped mirrors for fine tuning GDD compensation. With a total GDD of -540 fs^2, the SHG pulses are compressed down to 26 fs [red curve in Fig. 7(a)]. The black dashed curve in the same figure is the calculated autocorrelation trace of the corresponding TL pulses. The TL pulses have a duration of 24 fs, and the dechirped pulses are close to be transform-limited. We measure the average power stability of 64-W compressed pulses over 30 minutes and the RMS of average power is below 0.42% [Fig. 7(b)]. The inset of Fig. 7(b) shows a Gaussian-like spatial profile, indicating an excellent beam quality. The reduction in beam ellipticity (compared to the spot of the front-end laser) is attributed to minor mode mismatch within the MPC under high-power conditions.

https://doi.org/10.1017/hpl.2025.10056 Published online by Cambridge University Press

Figure 7. (a) Measured autocorrelation trace (red) and calculated autocorrelation trace of the TL pulse (black dashed). Inset: SHG spectrum. (b) Average power stability of the compressed SH pulses. Inset: SHG beam profile.

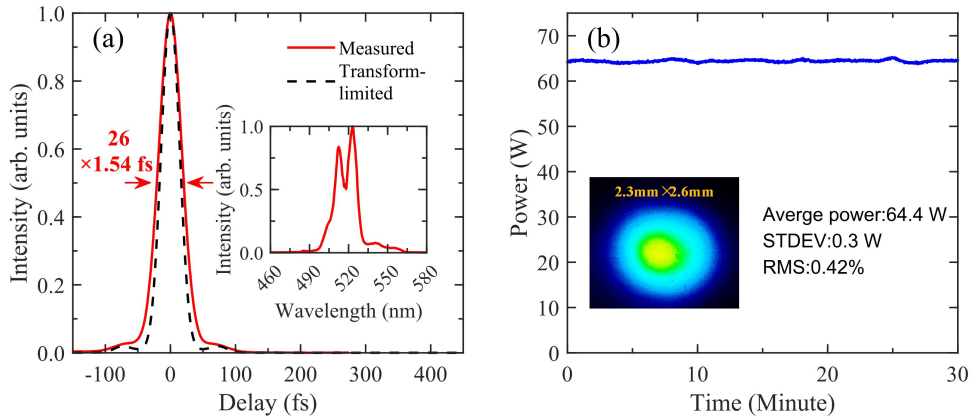

4. Conclusion

We implement a powerful ultrafast HHG driving source at the green wavelength, which is based on a Yb-fiber laser system that emits 1-MHz, 200-W, 230-fs pulses centered at 1.03 μm. These pulses are shortened by a MPC compressor and then frequency doubled in a BBO crystal. Centered at the green wavelength range, the generated SHG pulses are 26 fs in duration with 64-W average power (corresponding to 64-μJ pulse energy). Ongoing work is to employ this green source to drive HHG to produce EUV pulses with mW average power.

In recent years, the rapid development of high-power Yb-fiber laser systems [26] and high-power MPC compression technology has made it possible to obtain 1004-W, 31-fs pulses at 1.03 μm [17]. Frequency doubling at kW power level in BBO causes a thermal gradient that in turn degrades the beam quality [27, 28]. Bonding sapphire with large thermal conductivity can effectively mitigate the thermal effect of the

https://doi.org/10.1017/hpl.2025.10056 Published online by Cambridge University Press

crystal without compromising the SHG efficiency. As a result, it is feasible to produce green pulses with <30-fs duration and hundreds of Watts average power, which constitutes an enabling HHG driving source to achieve high-flux EUV pulses.

Acknowledgement

This work is supported by the Key Deployment Special Research Project of the Chinese Academy of Sciences (No. PTYQ2022YZ0001) and the National Natural Science Foundation of China (Nos. 62175255, 62227822).

Reference

1. M. Keunecke, C. Moller, D. Schmitt, H. Nolte, G. S. M. Jansen, M. Reutzel, M. Gutberlet, G. Halasi, D. Steil, S. Steil, and S. Mathias, "Time-resolved momentum microscopy with a 1 MHz high-harmonic extreme ultraviolet beamline," Review of Scientific Instruments 91, 063905 (2020). DOI: https://doi.org/10.1063/5.0006531
2. A. Mcpherson, G. Gibson, H. Jara, U. Johann, T. S. Luk, I. A. Mcintyre, K. Boyer, and C. K. Rhodes, "Studies of Multiphoton Production of Vacuum Ultraviolet-Radiation in the Rare-Gases," J Opt Soc Am B 4, 595-601 (1987). DOI: https://doi.org/10.1364/Josab.4.000595
3. M. Ferray, A. Lhuillier, X. F. Li, L. A. Lompre, G. Mainfray, and C. Manus, "Multiple-Harmonic Conversion of 1064-Nm Radiation in Rare-Gases," J Phys B-at Mol Opt 21, L31-L35 (1988). DOI: https://doi.org/10.1088/0953-4075/21/3/001
4. A. D. Shiner, C. Trallero-Herrero, N. Kajumba, H. C. Bandulet, D. Comtois, F. Legare, M. Giguere, J. C. Kieffer, P. B. Corkum, and D. M. Villeneuve, "Wavelength scaling of high harmonic generation efficiency," Physical Review Letters 103, 073902 (2009). DOI: https://doi.org/10.1103/PhysRevLett.103.073902
5. R. Klas, S. Demmler, M. Tschernajew, S. Hädrich, Y. Shamir, A. Tünnermann, J. Rothhardt, and J. Limpert, "Table-top milliwatt-class extreme ultraviolet high harmonic light source," Optica 3, 1167-1170 (2016). DOI: https://doi.org/10.1364/Optica.3.001167
6. A. Comby, D. Descamps, S. Beauvarlet, A. Gonzalez, F. Guichard, S. Petit, Y. Zaouter, and Y. Mairesse, "Cascaded harmonic generation from a fiber laser: a milliwatt XUV source," Opt. Express 27, 20383-20396 (2019). DOI: https://doi.org/10.1364/OE.27.020383
7. R. Klas, A. Kirsche, M. Gebhardt, J. Buldt, H. Stark, S. Hädrich, J. Rothhardt, and J. Limpert, "Ultra-short-pulse high-average-power

https://doi.org/10.1017/hpl.2025.10056 Published online by Cambridge University Press

megahertz-repetition-rate coherent extreme-ultraviolet light source," Photonix 2, 1-8 (2021). DOI: https://doi.org/10.1186/s43074-021-00028-y

8. J. Lee, D. R. Carlson, and R. J. Jones, "Optimizing intracavity high harmonic generation for XUV fs frequency combs," Opt. Express 19, 23315-23326 (2011). DOI: https://doi.org/10.1364/OE.19.023315
9. G. Chang and Z. Wei, "Ultrafast Fiber Lasers: An Expanding Versatile Toolbox," iScience 23, 101101 (2020). DOI: https://doi.org/10.1016/j.isci.2020.101101
10. M. Muller, C. Aleshire, A. Klenke, E. Haddad, F. Legare, A. Tunnermann, and J. Limpert, "10.4 kW coherently combined ultrafast fiber laser," Opt. Lett. 45, 3083-3086 (2020). DOI: https://doi.org/10.1364/OL.392843
11. V. Hilbert, M. Tschernajew, R. Klas, J. Limpert, and J. Rothhardt, "A compact, turnkey, narrow-bandwidth, tunable, and high-photon-flux extreme ultraviolet source," AIP Advances 10(2020). DOI: https://doi.org/10.1063/1.5133154
12. S. Wang, J. Yan, S. Song, A. Atanassov, Z. Wu, W. Brunner, D. Popmintchev, and T. Popmintchev, "High-performance ultrafast pulse compression in the visible spectral range for extreme nonlinear optics at kHz-MHz repetition rates," arXiv preprint arXiv:2307.01164 (2023). DOI: https://doi.org/10.48550/arXiv.2307.01164
13. J. Xia, C. Altucci, S. Amoruso, R. Bruzzese, R. Velotta, and X. Wang, "Generation of high energy, 30 fs pulses at 527 nm by hollow-fiber compression technique," Opt. Express 16, 3527-3536 (2008). DOI: https://doi.org/10.1364/oe.16.003527
14. D. Descamps, F. Guichard, S. Petit, S. Beauvarlet, A. Comby, L. Lavenu, and Y. Zaouter, "High-power sub-15 fs nonlinear pulse compression at 515 nm of an ultrafast Yb-doped fiber amplifier," Opt. Lett. 46, 1804-1807 (2021). DOI: https://doi.org/10.1364/OL.419683
15. S. Hädrich, A. Klenke, A. Hoffmann, T. Eidam, T. Gottschall, J. Rothhardt, J. Limpert, and A. Tünnermann, "Nonlinear compression to sub-30-fs, 0.5 mJ pulses at 135 W of average power," Opt. Lett. 38, 3866-3869 (2013). DOI: https://doi.org/10.1364/OL.38.003866
16. T. Nagy, S. Hädrich, P. Simon, A. Blumenstein, N. Walther, R. Klas, J. Buldt, H. Stark, S. Breitkopf, P. Jójárt, I. Seres, Z. Várallyay, T. Eidam, and J. Limpert, "Generation of three-cycle multi-millijoule laser pulses at 318 W average power," Optica 6, 1423-1424 (2019). DOI: https://doi.org/10.1364/OPTICA.6.001423
17. C. Grebing, M. Müller, J. Buldt, H. Stark, and J. Limpert, "Kilowatt-average-power compression of millijoule pulses in a gas-filled multi-pass cell," Opt. Lett. 45, 6250-6253 (2020). DOI: https://doi.org/10.1364/OL.408998
18. V. Hariton, A. Bin Wahid, G. Figueira, K. Fritsch, and O. Pronin, "Multipass spectral broadening and compression in the green spectral range," Opt. Lett. 47, 1246-1249 (2022). DOI: https://doi.org/10.1364/OL.450200
19. M. Karst, P. Pfaller, R. Klas, Z. Wang, P. Gierschke, J. Rothhardt, and J.

https://doi.org/10.1017/hpl.2025.10056 Published online by Cambridge University Press

Limpert, "22-W average power high pulse energy multipass-cell-based post-compression in the green spectral range," Opt. Lett. 48, 1300-1303 (2023). DOI: https://doi.org/10.1364/OL.482600

20. N. V. Didenko, A. V. Konyashchenko, L. L. Losev, V. S. Pazyuk, and S. Y. Tenyakov, "Femtosecond pulse compression based on second harmonic generation from a frequency chirped pulse," Optics Communications 282, 997-999 (2009). DOI: https://doi.org/10.1016/j.optcom.2008.11.010
21. N. V. Didenko, A. V. Konyashchenko, P. V. Kostryukov, L. L. Losev, and S. Y. Tenyakov, "Second harmonic generation of spectrally broadened femtosecond ytterbium laser radiation in a gas-filled capillary," Quantum Electronics 41, 804-808 (2011). DOI: https://doi.org/10.1070/QE2011v041n09ABEH014632
22. R. Riedel, J. Rothhardt, K. Beil, B. Gronloh, A. Klenke, H. Hoppner, M. Schulz, U. Teubner, C. Krankel, J. Limpert, A. Tunnermann, M. J. Prandolini, and F. Tavella, "Thermal properties of borate crystals for high power optical parametric chirped-pulse amplification," Opt. Express 22, 17607-17619 (2014). DOI: https://doi.org/10.1364/OE.22.017607
23. D.-L. Wang, Z. Shi, J.-S. Wang, H.-Y. Wu, X.-H. Zhang, and G.-Q. Chang, "1 MHz, 273 W average power Ytterbium-doped rod-type fiber chirped pulse amplification system," Acta Physica Sinica 73, 134204 (2024). DOI: https://doi.org/10.7498/aps.73.20240300
24. H. Yoshida, H. Fujita, M. Nakatsuka, M. Yoshimura, T. Sasaki, T. Kamimura, and K. Yoshida, "Dependences of Laser-Induced Bulk Damage Threshold and Crack Patterns in Several Nonlinear Crystals on Irradiation Direction," Japanese Journal of Applied Physics 45, 766 (2006). DOI: https://doi.org/10.1143/JJAP.45.766
25. A. L. Viotti, M. Seidel, E. Escoto, S. Rajhans, W. P. Leemans, I. Hartl, and C. M. Heyl, "Multi-pass cells for post-compression of ultrashort laser pulses," Optica 9, 197-216 (2022). DOI: https://doi.org/10.1364/Optica.449225
26. H. Fathi, M. Naerhi, and R. Gumenyuk, "Towards Ultimate High-Power Scaling: Coherent Beam Combining of Fiber Lasers," Photonics-Basel 8, 566 (2021). DOI: https://doi.org/10.3390/photonics8120566
27. C. Rothhardt, J. Rothhardt, A. Klenke, T. Peschel, R. Eberhardt, J. Limpert, and A. Tünnermann, "BBO-sapphire sandwich structure for frequency conversion of high power lasers," Optical Materials Express 4, 1092-1103 (2014). DOI: https://doi.org/10.1364/Ome.4.001092
28. J. Rothhardt, C. Rothhardt, M. Muller, A. Klenke, M. Kienel, S. Demmler, T. Elsmann, M. Rothhardt, J. Limpert, and A. Tunnermann, "100 W average power femtosecond laser at 343 nm," Opt. Lett. 41, 1885-1888 (2016). DOI: https://doi.org/10.1364/OL.41.001885

https://doi.org/10.1017/hpl.2025.10056 Published online by Cambridge University Press